ELSEVIER

Thermochimica Acta 299 (1997) 101–108

thermochimica acta

The extraction of phonon and electron properties from experimental heat capacity with new approximation based on high temperature expansion

Victor N. Naumov[a], Galina I. Frolova[a,*], Tooru Atake[b]

[a] *Institute of Inorganic Chemistry, Lavrentiev Avenue, 3, Siberian Branch of Russian Acad. of Sci., 630090, Novosibirsk, Russia*
[b] *Tokyo Institute of Technology, Materials & Structures Laboratory, 4259 Nagatsuta, Midori, Yokohama 226, Japan*

Abstract

A new approach to the high temperature expansion of heat capacity $C(T)$ is proposed. The lattice heat capacity is described by two first terms of this expansion with characteristic temperatures (θ_2 and θ_4) plus a remainder. The latter is approximated by some function with only parameter θ_* which is attributed to the upper limit of a phonon spectrum.

This new form of expansion extends downwards along the range of a good approximation of a lattice heat capacity in comparison with ordinary truncated high temperature expansion. This, in turn, allows investigation of the new phenomena in some substances.

This method was tested on several model curves $C(T)$ with the phonon spectrum known in advance. The examples of the determination of phonon and electron characteristics for dielectrics, metals and high temperature superconductors are shown.

Keywords: Approximation of remainder; Electron heat capacity; Heat capacity of solids; High temperature expansion; Moments of phonon spectrum

1. Introduction

The investigation of the heat capacity of solids provides wide information about their characteristics and processes. To extract this information one separates heat capacity into contributions of different origins.

Ordinarily, the harmonic part of a lattice heat capacity makes the main contribution into entire heat capacity of solids. Other contributions into heat capacity have to be extracted against this large background; thus one should have the proper method for its description.

The lattice heat capacity of a crystal in harmonic approximation is a sum of contributions from separate normal vibrations, (see, for example, [1]):

$$C(T) = 3Nk \int_0^{\omega_{max}} \Psi\left(\frac{\hbar\omega}{kT}\right) g(\omega) d\omega;$$

$$\Psi(z) = \frac{z^2}{e^z + e^{-z} - 2}. \qquad (1)$$

Here $\Psi(z)$ is the Einstein function, $z = \hbar\omega/kT$, $g(\omega)$ is the normalized photon spectrum

$$\int_0^{\omega_{max}} g(\omega) d\omega = 1,$$

ω_{max} is the upper bound of a photon spectrum.

The high temperature expansion is often used for a description of this lattice heat capacity at moderate temperatures. This expansion is based

*Corresponding author. Fax: 7 3832 35 59 60; e-mail: ginzburg@math.nsc.ru.

PII S0040-6031(97)00143-3

on the Taylor series for the Einstein function $\Psi(z)$ in Eq. (1):

$$\Psi(z) = \sum_{n=0}^{\infty} A_n z^{2n} \tag{2}$$

$$A_1 = -\frac{1}{12},\ A_2 = \frac{1}{240},\ A_3 = -\frac{1}{6048},$$
$$A_4 = \frac{1}{17280}, \cdots$$

Substituting this expansion into the integral (1) we have

$$C(T) = 3Nk \int_0^{\omega_{max}} g(\omega) \sum_{n=0}^{\infty} (A_n z^{2n}) d\omega$$
$$\equiv 3Nk \sum_{n=0}^{\infty} A_n \int_0^{\omega_{max}} g(\omega) \left(\frac{\hbar\omega}{kT}\right)^{2n} d\omega.$$

The further integration over ω results in *the high temperature expansion of the heat capacity*:

$$C(T) = 3Nk \sum_{n=0}^{\infty} A_n \left(\frac{\hbar}{k}\right)^{2n} \frac{\mu_{2n}}{T^{2n}}. \tag{3}$$

Here μ_{2n} are the moments of a phonon spectrum,

$$\mu_{2n} = \int_0^{\omega_{max}} g(\omega)\omega^{2n} d\omega.$$

At high temperatures only one (the *zero*th) term of the series gives a good approximation for the harmonic part of a lattice heat capacity (the Dulong and Petit law). When temperature decreases, one needs to take into account the second, then the third and so on terms of the series to describe heat capacity.

Fig. 1 shows the contributions from each of the successive terms on high temperature expansion for the Debye heat capacity. It is seen that each following term extends the range of good approximation, but this becomes less and less.

In practice, one uses 3 or 4 first terms of the series and the remainder is discarded.

When analyzing the experimental data the considered coefficients are found as the varied parameters. Thus, one obtains both the moments of the photon spectrum μ_2, μ_4,... and the good approximation for the harmonic lattice heat capacity in some temperature interval.

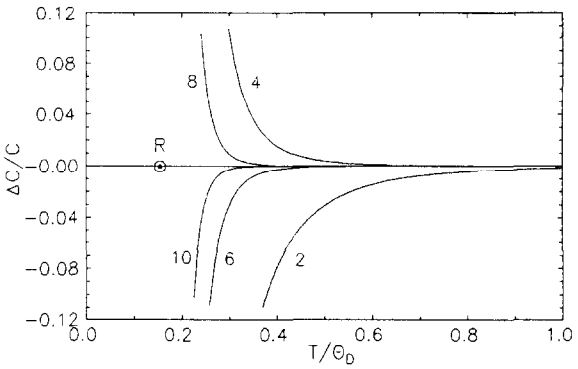

Fig. 1. The difference between the true Debye heat capacity and calculated one by Eq. (3) with a different number of terms: 2 – with μ_2; 4 – with μ_2 and μ_4; 6 – with μ_2, μ_4 and μ_6.

This approximating scheme was used, for example, in papers [2–5].

The successive terms of the high temperature series (3) go into infinity when temperature goes to zero. Therefore the range of the discussed approximation is bounded in temperature from below.

Besides, when the temperature increases, the harmonic lattice heat capacity rises less and less progressively. Against this background the other contributions to the total heat capacity become essential (anharmonicity [6], electron heat capacity in metals,...). Without taking them into account the range of good approximation by means of the above series (3) is also bounded from the above, typically, by temperatures $T <\sim 0.5\Theta_D$. In such a case the range of good approximation is rather narrow ($0.35\Theta_D - 0.5\Theta_D$), and the statistical accuracy of obtained results is not very high. The addition of a linear term γT to the left side of expansion (3) allows one to extend the range of good approximation upwards. Such an approach was used in Refs. [4,6,7].

In the present paper the method that allows one to extend the range of good approximation downwards is expounded [7].

The idea of this method consists of the fact that even a rough approximation of a remainder of the series extends well downwards the range of good description of heat capacity.

2. Description of the method

For the description of the proposed method it is convenient to introduce the characteristic temperatures related to the $2n$th moments of the phonon spectrum:

$$\theta_{2n} = \frac{\hbar}{k}\sqrt[2n]{\mu_{2n}}.$$

In terms of characteristic temperatures the above high temperature expansion (3) has the form

$$C(T) = 3Nk\sum_{n=0}^{\infty} A_n\left(\frac{\theta_{2n}}{T}\right)^{2n} = 3Nk\left[1 + A_1\left(\frac{\theta_2}{T}\right)^2 + A_2\left(\frac{\theta_4}{T}\right)^4 + \cdots\right]. \tag{4}$$

This equation can be presented as the sum of the first $m+1$ terms plus remainder R_m:

$$C(T) = 3Nk\sum_{n=0}^{m} A_n\left(\frac{\theta_{2n}}{T}\right)^{2n} + R_m; \tag{5}$$

$$R_m = 3Nk\sum_{n=m+1}^{\infty} A_n\left(\frac{\theta_{2n}}{T}\right)^{2n}.$$

This exact expression for the heat capacity is a basic one for the following approximations.

For any spectrum $g(\omega)$ the distribution of the characteristic temperatures θ_{2n} is of the form shown in Fig. 2. These characteristic temperatures tend monotonically to the upper boundary of the phonon spectrum $\theta_{\text{bound}} = \hbar\omega_{\max}/k$.

Such behaviour of the values θ_{2n} leads us to the idea to replace them by one characteristic temperature θ_*. It was convenient to replace all θ_{2n} in remainder R_m by

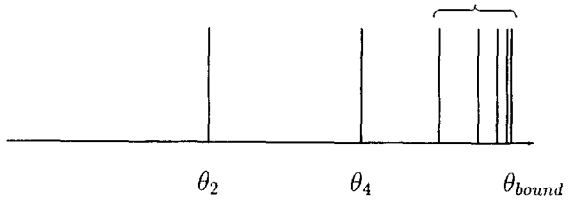

Fig. 2. Schematic distribution of characteristic temperatures θ_{2n}.

substitution

$$\theta_{2n}^{2n} \Rightarrow \theta_*^{2n-2m}\theta_{2m}^{2m}. \tag{6}$$

This substitution transforms the above equation for the heat capacity (Eq. (5)) into its approximated form:

$$C(T) \approx 3NK\left\{\sum_{n=0}^{m-1} A_n\left(\frac{\theta_{2n}}{T}\right)^{2n} + \left(\frac{\theta_{2m}}{\theta_*}\right)^{2m}\sum_{n=m}^{\infty} A_n x^{2n}\right\}; \tag{7}$$

$$\left(x = \frac{\theta_*}{T}\right).$$

In the particular case $m = 2$ we have $\theta_{2n}^{2n} \Rightarrow \theta_*^{2n-4}\theta_4^4$. Then Eq. (7) is of the form

$$C(T) \approx 3Nk\left\{1 + A_1\left(\frac{\theta_2}{T}\right)^2 + \left(\frac{\theta_4}{\theta_*}\right)^4 \cdot \sum_{n=2}^{\infty} A_n x^{2n}\right\}.$$

The infinite sum in the right side of this equation can be expressed via the Einstein function $\Psi(x)$ (1,2) as

$$\sum_{n=2}^{\infty} A_n x^{2n} = \Psi(x) - 1 - A_1 x^2.$$

Finally, we obtain the equation *for the approximation of the harmonic part of the lattice heat capacity in the proposed method*:

$$\frac{C(T)}{3Nk} \approx 1 + A_1\left(\frac{\theta_2}{T}\right)^2 + \left(\frac{\theta_4}{\theta_*}\right)^4 \cdot \left[\Psi\left(\frac{\theta_*}{T}\right) - 1 - A_1\left(\frac{\theta_*}{T}\right)^2\right]. \tag{8}$$

It contains three varied parameters θ_2, θ_4 and θ_*. The latter is close to the upper boundary of the phonon spectrum θ_{bound}, as it is seen in Fig. 2.

This form is used in our approximations. The final equation for case $m = 3$ can be obtained in a similar way.

As an example we approximated the Debye heat capacity as an 'experimental' one by Eq. (7) with $m = 2$ and $m = 3$. The parameters θ_2, θ_4, θ_6, θ_* were obtained by variation. These parameters, and those directly calculated from the Debye density of states are presented in the Table 1. Besides, the 'more realistic' density of states (Fig. 3) was treated, and

Table 1
The characteristic temperatures for the model phonon spectra

n	Debye spectrum		Spectrum of Fig. 3	
	θ_{2n}/θ_D from spectrum	θ_{2n}/θ_D from heat capacity	$\theta_{2n}/\theta_{bound}$	$\theta_{2n}/\theta_{bound}$ from heat capacity
1	0.77460	0.77460	0.56586	0.56584
2	0.80911	0.80899	0.62118	0.62078
*	—	0.87758	—	0.74013

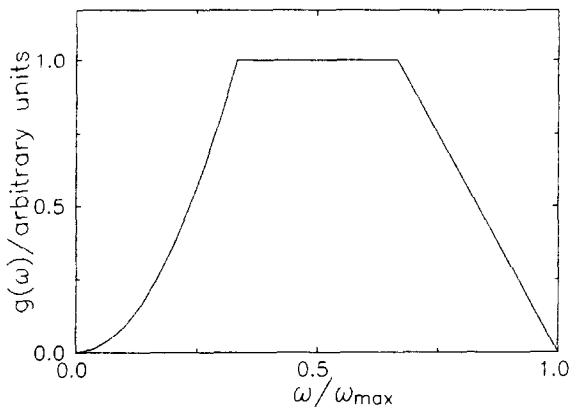

Fig. 3. The model phonon spectrum.

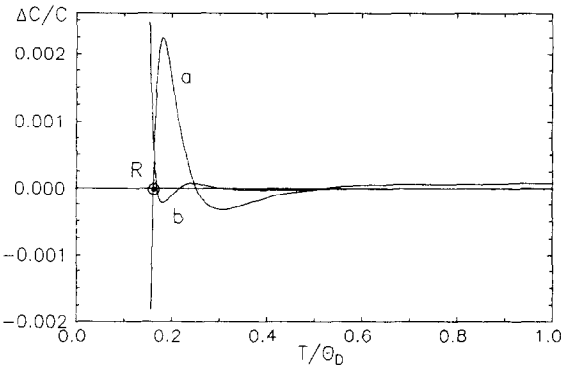

Fig. 4. The difference between the true Debye heat capacity and the approximated one by Eq. (8). Curve (a): $m = 2$; curve (b): $m = 3$.

the results are presented in the same table. In both cases the values of θ_2 obtained from the heat capacity and those calculated from the density of states coincide with very high accuracy. The differences in values of θ_4 are also very small (less than 0.06%).

The differences between the true Debye heat capacity and approximated ones are shown in Fig. 4. The curve (a) is described by the set of parameters θ_2, θ_4 and θ_*. In the range from θ_D to 0.165 θ_D it deviates from the true Debye heat capacity by less than 0.25%. Moreover, it deviates from the true Debye heat capacity by less than 0.01% within the interval $0.25\theta_D - \theta_D$. The comparison with Fig. 1 (where the truncated series is presented) shows that our approximation of the remainder extends sharply the interval of a good approximation. The curve (b) is described by the set of parameters θ_2, θ_4, θ_6 and θ_*. Its deviation from the true Debye heat capacity does not exceed 0.025% within the same range $0.165\theta_D - \theta_D$. One can conclude that this next iteration shifts the lower boundary of precise description downwards from $0.250\theta_D$ to $0.165\theta_D$ (with accuracy better than 0.025%). It improves the accuracy of description above $0.165\theta_D$ from 0.25% to 0.025%.

In many cases the contribution from the next iteration (with $m = 3$ and θ_6) is inside experimental accuracy. So, the approximation with $m = 2$ (with three parameters θ_2, θ_4 and θ_*) is sufficient.

3. Applications

The method was successfully applied for the analysis of the heat capacity of many substances.

To show the results in a convenient form in a graph we used the special coordinates X and Y:

$$Y(T, C) = -\frac{T^2}{A_1}\left[1 - \frac{C(T)}{3Nk}\right],$$

$$X(\theta_*, T) = \frac{T^2}{A_1} \cdot \frac{[1 + A_1 x^2 - \Psi(x)]}{\theta_*^4}. \qquad (9)$$

Here $\Psi(x)$ is the Einstein function (1), $(x = \theta_*/T)$.

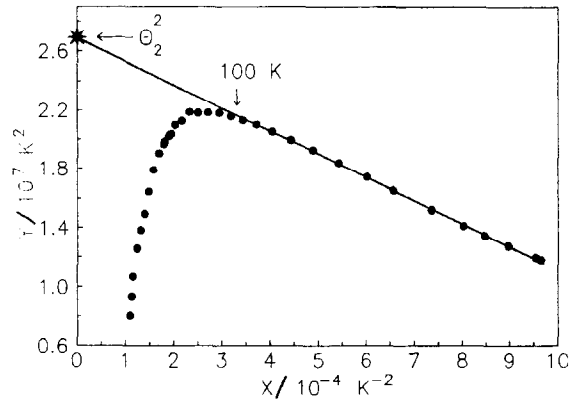

Fig. 5. The heat capacity of germanium tetraiodide (GeI_4) in coordinates X and Y [8].

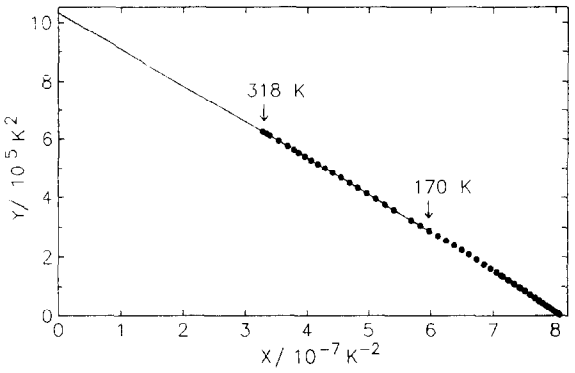

Fig. 6. The heat capacity of α-boron α-B in coordinates X and Y [9].

The dependence $Y(X)$ looks as a straight line

$$Y(T, C) = \theta_2^2 - \theta_4^4 X(\theta_*, T) \tag{10}$$

in the temperature region where the approximated harmonic lattice heat capacity (8) describes well the total heat capacity.

The intersection of this straight line with the axis of ordinates shows us θ_2 and its slope shows θ_4.

Eq. (10) was used to determine the parameters by least square method.

In Fig. 5 we show the approximation of the heat capacity for dielectric germanium tetraiodide (GeI_4) by expression (8).

It is seen that in these coordinates the lattice heat capacity looks like a straight line in the temperature interval 37–106 K. Above 106 K experimental points deviate from the straight line.

This deviation of points from the straight line displays the anharmonic contribution into the heat capacity of the compound. The temperature 106 K is the boundary of the range where the harmonic approximation for the heat capacity coincides with the total heat capacity within the experimental accuracy.

In Fig. 6 the dependence $Y(X)$ for α-boron is shown. It looks like a straight line in the temperature interval 182–318 K. Even at 300 K no anharmonicity is revealed. (This substance has very high Debye temperature).

The heat capacity of metals contains the linear contribution from conduction electrons. It can be taken into account by describing the lattice heat capacity as a difference between total heat capacity and electron one so that

$$C_{\text{latt}} = C_{\text{tot}} - \gamma T.$$

Then γ is the additional variable included in coordinate Y as follows:

$$Y(\gamma, T, C) = -\frac{T^2}{A_1}\left[1 - \frac{C(T) - \gamma T}{3Nk}\right],$$

and the above equation for $Y(X)$ has the same form as Eq. (10)

$$Y(\gamma, T, C) = \theta_2^2 - \theta_4^4 X(\theta_*, T). \tag{11}$$

It is a straight line in the range of validity of an approximation, and its intersection with the axis of ordinates shows us θ_2 and its slope shows θ_4.

When we know the optimal parameters θ_2, θ_4 and θ_*, we can calculate the harmonic lattice heat capacity by the above final Eq. (8). Then other contributions can be obtained as a difference between the total heat capacity and the calculated heat capacity. Of course, it is necessary to do further analysis of these extracted contributions.

In Fig. 7 we present the difference between the experimental heat capacity and calculated harmonic lattice heat capacity of mercury. The parameters of the harmonic lattice heat capacity were found in the temperature interval 18–44 K.

This difference can be considered as the sum of electron heat capacity and anharmonic one. As has been stated above further analysis should be done.

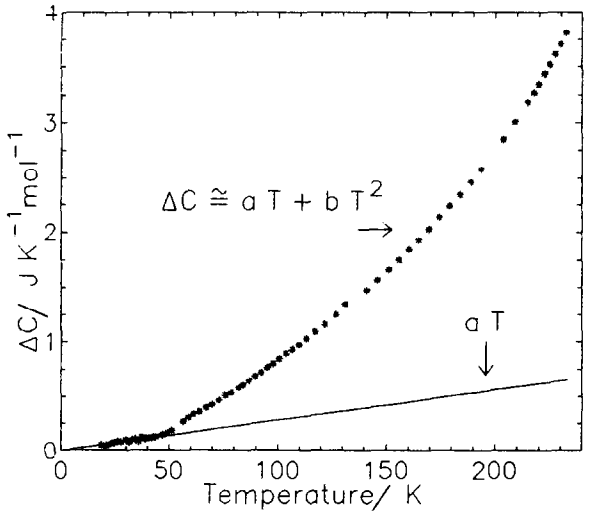

Fig. 7. The difference between the experimental heat capacity and the lattice one for mercury (Hg) [16].

The electron heat capacity is not the only linear contribution into the total heat capacity of crystal. In the wide temperature interval the anharmonic contribution is also linear in temperature, AT. Therefore, the final equation for the approximation, while taking into account both electron component and linear anharmonic one, has a form

$$C(T) \approx (\gamma + A)T + 3Nk\left\{1 + A_1\left(\frac{\theta_2}{T}\right)^2 + \left(\frac{\theta_4}{\theta_*}\right)^4 \cdot \left[\Psi\left(\frac{\theta_*}{T}\right) - 1 - A_1\left(\frac{\theta_*}{T}\right)^2\right]\right\}. \quad (12)$$

It contains four varied parameters θ_2, θ_4, θ_* and $\gamma + A$.

Table 2 shows the characteristic temperatures and coefficients of the linear component of heat capacity for some dielectrics. We obtained small linear contributions into the heat capacity of dielectrics $ZrTe_5$ [10] and $KY(MoO_4)_2$ [11] which may correspond to the anharmonic contribution.

In Table 3 the characteristic temperatures and the coefficients of linear component are presented for some metals. The parameters θ_2 and the coefficients of linear contribution $\gamma + A$ for copper and gold were found to be in agreement with those obtained earlier [4].

This method was also applied for the determination of phonon and electron characteristics of high temperature superconductors. The results of analysis are presented in Table 4.

In Fig. 8 the harmonic lattice heat capacity of HoBCO is shown in above coordinates X and Y.

Table 2
Phonon characteristic temperatures and coefficients of linear component of heat capacity for some dielectrics. Errors are statistical. ΔT is the interval of approximation and $\gamma + A$ is in mJ/mol K^2

	GeI_4 [8]	α-boron [9]	$ZrTe_5$ [10]	$KY(MoO_4)_2$ [11]
ΔT K	37–106	182–314	27–98	121–289
θ_2 K	164 ± 1.5	1016 ± 2	176 ± 0.7	594 ± 3
θ_4 K	200 ± 4	1056 ± 4	194.6 ± 1.4	716.5 ± 3.5
θ_* K	235 ± 8	1113 ± 9	222 ± 2.5	904 ± 9
$\gamma + A$	—	—	0.43 ± 0.15	0.4 ± 0.1

Table 3
Phonon characteristic temperatures and coefficients of linear component of heat capacity for some metals. Errors are statistical. ΔT is the interval of approximation and $\gamma + A$ is in mJ/mol K^2

	Cu [12,13]	Au [14,15]	Hg [16]	Rh [17]	Ir [17]
ΔT K	47–129	24–81	18–44	25–150	20–115
θ_2 K	247.6 ± 0.6	142 ± 1	88.8 ± 0.3	266.3 ± 0.6	221.0 ± 0.7
θ_4 K	259.5 ± 2.5	151 ± 1	100.7 ± 0.5	275.0 ± 1.5	228 ± 2
θ_* K	279 ± 4	166 ± 3	118.0 ± 1.5	287 ± 3	238 ± 3
$\gamma + A$	2.4 ± 0.1	1.0 ± 0.2	2.8 ± 0.2	(4.65)	(3.51)

Table 4
Phonon characteristic temperatures and coefficients of linear component of heat capacity for some high temperature superconductors. Errors are statistical. ΔT is the interval of approximation and $\gamma + A$ is in mJ/mol K^2

	HoBCO [18]	HoBCO [19]	TmBCO [20]	DyBCO [21]
ΔT K	92–236	100–232	100–260	100–290
θ_2 K	427 ± 3	430 ± 9	429 ± 2	436 ± 1
θ_4 K	484 ± 4	486 ± 15	486 ± 4	504 ± 3
θ_* K	569 ± 8	570 ± 30	595 ± 8	610 ± 5
$\gamma + A$	38 ± 3	35 ± 6	38 ± 1.5	39.4 ± 0.7

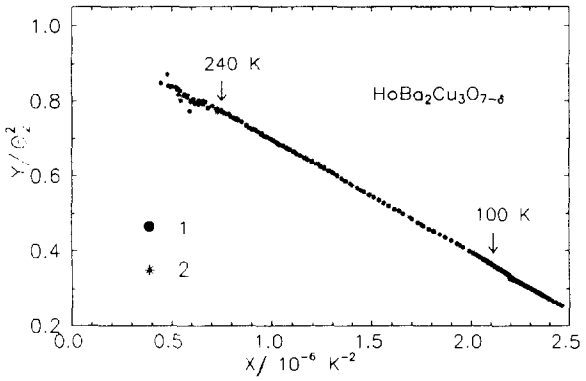

Fig. 8. The lattice heat capacity of HoBCO in coordinates X and Y. The experimental are data from Refs. [18,19].

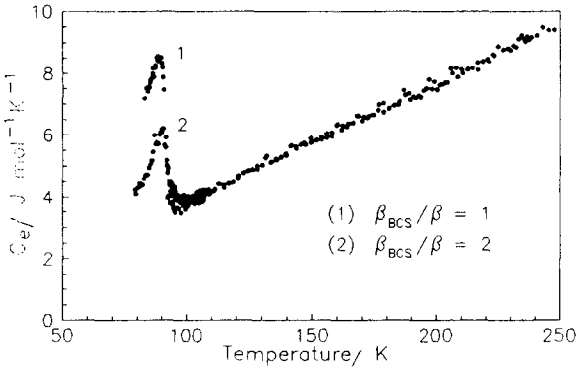

Fig. 9. Electron heat capacity of HoBCO and TmBCO. 1 – curve for TmBCO [20]; 2 – two curves for HoBCO with data from Refs. [18,19].

The experimental data were obtained from Refs. [18,19]. The points from both these experiments in the temperature range 100–300 K fall very well on the straight line.

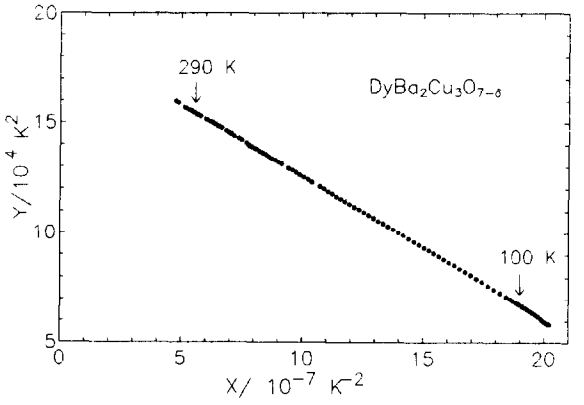

Fig. 10. The lattice heat capacity of DyBCO in coordinates X and Y. The experimental data from Ref. [21].

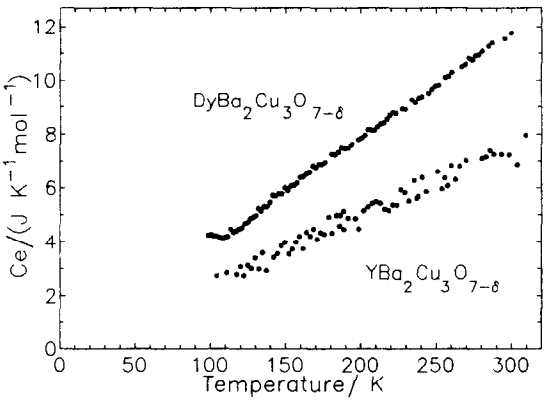

Fig. 11. Electron heat capacity of DyBCO [21].

In Fig. 9 the electron component of heat capacity HoBCO is shown. It has been obtained as a difference between the total heat capacity and the harmonic lattice one. Here curve 1 is for TmBCO [20] and curve 2 is for HoBCO [18,19] (coincided).

In Fig. 10 the harmonic lattice heat capacity of DyBCO from the paper [21] is shown in the above coordinates X and Y. In Fig. 11 the electron component of heat capacity of DyBCO is shown. It has been obtained as a difference between the total heat capacity and the harmonic lattice one.

4. Conclusion

In this work a new approach is proposed for the analysis of the heat capacity of solids based on the high temperature expansion of harmonic heat capacity. It allows one to extend the range of a good approximation well downwards in comparison with ordinary high temperature expansion. The harmonic heat capacity is described by two (or three) first terms of this expansion (with characteristic temperatures θ_2 and θ_4) plus some specific form of the remainder. The latter is approximated by a known function with the only new parameter θ_*.

This approach allows one to analyse the experimental data of a wide set of substances and to extract both the parameters of phonon spectrum and the other contributions into the heat capacity. The above examples show that Eq. (8) is a good experiment for this goal. Of course, the other contributions are the subject of the additional analysis in accordance with the physical problem which is going to be investigated.

References

[1] L.A. Girifalco, Statistical Physics of Materials, Wiley-Interscience Pub. New York, London, Sydney, Toronto (1973).
[2] T.H. Barron, W.T. Berg and J.A. Morrison, Proc. Roy. Soc., A242 (1957) 478.
[3] V.V. Korshunov, Fizika Metallov i Metallovedenie, 41 (1976) 292 (in Russian).
[4] C.S. Knapp, S.O. Bader and Z. Fisk, Phys. Rev., B13 (1976) 3783.
[5] V.N. Naumov, I.E. Paukov, G.P. Ramanauskas and V. Ja. Chechovskoy, Zhurnal Fizicheskoy Khimii 62 (1988) 25 (in Russian).
[6] G. Liebfried, W. Ludwig, Theory of Anharmonic Effects in Crystals, Academic Press Inc., New York, London (1961).
[7] V.N. Naumov, Phys. Rev., B49 (1994) 13247.
[8] I.E. Paukov, Yu.F. Minenkov, V.N. Naumov, L.N. Zelenina, Zhurn. Fiz. Khimii, in press (in Russian).
[9] V.N. Naumov, V.V. Nogteva, I.E. Paukov, G.V. Tsagareishvili, Zhurn. Fiz. Khimii, 71 (1997) 1596 (in Russian).
[10] R. Shaviv and E.F. Westrum Jr.H. Fjellvåg and A. Kjekshus, J. Sol. St. Chem., 81 (1989) 183.
[11] G.I. Frolova, L.P. Kozeeva, I.E. Paukov, Zhurn. Fiz. Khimii, 57 (1983) 1802 (in Russian).
[12] A.N. Kovryanov, Yu.R. Chashkin, V.A. Rabinovich. In Teplofizicheskie svoistva veschestv i materialov, Nauka, Moscow (1980) 136 (in Russian).
[13] D.L. Martin, Can. J. of Physics, 38 (1960) 17.
[14] P. Franzosini and K. Glusius, Z. Naturforsch., 18a (1963) 1243.
[15] T.H. Geballe and W.F. Gianque, J. Am. Chem. Soc., 74 (1952) 2368.
[16] E.B. Amitin, E.G. Lebedeva and I.E. Paukov, Zh. Fiz. Khimii, 53 (1979) 2666.
[17] G.T. Furukawa, M.R. Reilly and J.S. Gallagher, J. Phys. Chem. Ref. Data, 3 (1974) 163.
[18] T. Atake, O.Z. Zhang, Y. Takagi, Y. Saito, Report Research Lab. of Engineering Materials, Tokyo Inst. of Technology (1989) 11.
[19] V.N. Naumov, G.I. Frolova, E.B. Amitin, V.E. Fedorov and P.P. Samoilov, Physica, C 262 (1996) 143.
[20] T. Atake, H. Kawaji, S. Takanabe, Y. Saito, K. Mori and Y. Sacki, Thermochim. Acta, 139 (1989) 169.
[21] T. Atake, Y. Takagi, T. Nakamura and Y. Saito, Phys. Rev., B37 (1988) 552.